Sensitivity Analysis of the Mascaret model on the Odet River

Anne-Laure Tiberi-Wadier, Nicole Goutal, Sophie Ricci, Philippe Sergent, Céline Monteil

Sensitivity Analysis of the Mascaret model on the Odet River

Anne-Laure Tiberi-Wadier*, Nicole Goutal†, Sophie Ricci‡, Philippe Sergent§ and Céline Monteil¶
*Cerema Eau, Mer et Fleuves, Plouzané, France, Anne-Laure.Tiberi-Wadier@cerema.fr
†EDF R&D et Laboratoire d'Hydraulique Saint-Venant, Chatou, France, nicole.goutal@edf.fr
‡CECI, UMR5318, CNRS/CERFACS, Toulouse, France, ricci@cerfacs.com
§Cerema Eau, Mer et Fleuves, Margny-Les-compiègne, France, Philippe.Sergent@cerema.fr
¶EDF R&D, Chatou, France

***Abstract*—A Global Sensitivity Analysis (GSA) is carried out on the Mascaret model of the Odet river (France, Brittany) to identify and rank the major sources of uncertainty at observing stations on the network for the simulated water level, considering the upstream and downstream boundary conditions and the area distributed friction coefficients values. Upstream, ensemble hydrologic forcings are forecasted with the rainfall-runoff distributed model MORDOR-TS, using uncertain hydrologic model parameters drawn from uniform distributions. The downstream maritime boundary condition is perturbed taking into account the temporal correlation of the errors in storm surge. The Sobol' indices are computed at Kervir, Moulin-Vert and Justice stations given hypothesis on the statistical distribution of the aleatory variables.**

The study focuses on the 23 to the 26 December 2013 event. GSA highlights that the simulated water level at the three stations is mainly controlled by the immediate downstream friction coefficient when the boundary conditions are not perturbed. The flood plain friction coefficients only become important around the peak of the event. However, when the boundary conditions are also taken into account, they become predominant for the simulated water level and the value of the friction coefficients has less influence.

I. Introduction

SCHAPI and SPC (i.e. flood forecasting services) use day-to-day deterministic hydrologic and hydraulic models forced by precipitation forecasts. Input and parameters to these models are uncertain, thus limiting the reliability of a deterministic discharge forecast. An ensemble approach should be thus favoured. The cascade of uncertainty in a chained ensemble framework is being investigated on the Odet catchment, in the North-West of France in Brittany.

The hydrodynamics of the river is simulated with the 1D solver MASCARET. This model is used daily by the SCP VCB (Vilaine et Côtiers Bretons) for flood forecasting in the city of Quimper. However, the geometry of the model has been modified here for a better numerical stability and a new calibration has been done. The model used in this study is thus not exactly the operational model. Ensemble hydrologic forcings are forecasted with the rainfall-runoff distributed model MORDOR-TS, using uncertain hydrologic model parameters drawn from uniform distributions.

A Global Sensitivity Analysis (GSA) on the hydraulic model is carried out in order to identify and rank the major sources of uncertainties in water level, considering uncertainties in the upstream and downstream boundary conditions and the area distributed friction parameters values (K_s).

The article is organized as follows. Section II presents the catchment study and the areas represented by the hydrologic and hydraulic models. Section III presents the data sets used in the study. Section IV describes the calibration of the MORDOR-TS model, and the construction of the Hydrologic Ensemble Forecasts (HEF). Section V is devoted to the calibration of the Mascaret model. The GSA is presented in section VI, and the associated results are given in section VII. Conclusion and perspectives are finally given in section VIII.

II. Presentation of the study area

The Odet river is a coastal river located in Western Britany. It flows through the city of Quimper, then South to the sea (Fig 1). Astronomical tide ranges between 1.40 m and 5.55 m at the mouth at Plaisance. The Odet catchment area is 720 km^2, for a total length of about 60 km for the Odet river. The Jet and Steir rivers are two tributaries of the Odet river.

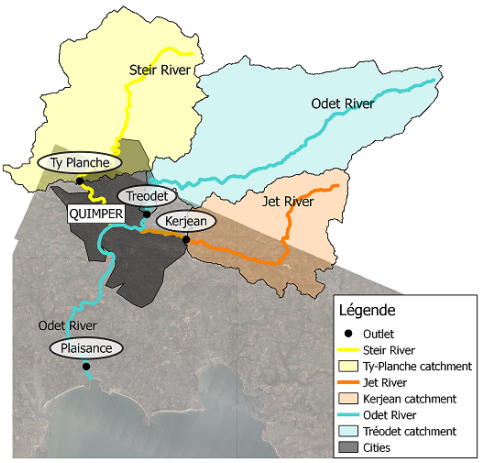

Fig. 1: The rivers Odet, Steir and Jet with the location of the hydrologic stations.

A. Hydrologic modeling

The MORDOR-TS rainfall-runoff model provides hydrologic streamflows on each of the three upstream subcatchments

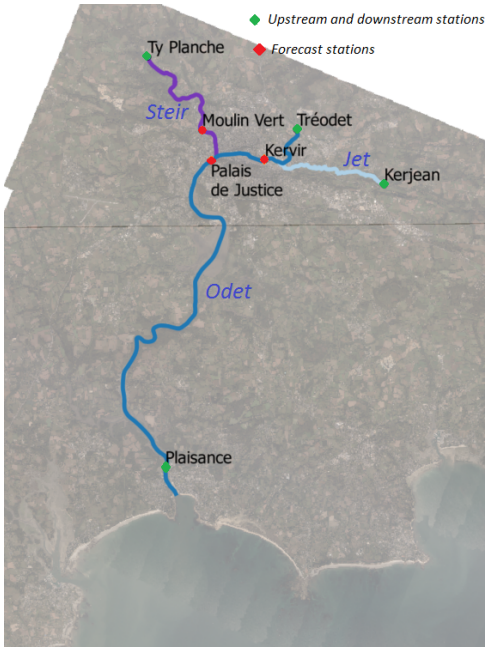

Fig. 2: Parts of the rivers covered by the Mascaret model.

which exutories are named Tréodet, Kerjean and Ty Planche (Fig 1). Table I summarizes the characteristics of the upstream subcatchments.

B. Hydraulic modeling

Mascaret is a 1D model based on Saint-Venant equations. The Mascaret model covers the downstream part of the catchement and focuses on urban areas as shown on Figure 2. It aims at forecasting the water level at three observing stations Kervir, Justice (river Odet) and Moulin Vert (river Steir), represented in red in figure 2. The upstream and downstream stations of the hydraulic model are represented in green. The length of the reaches are about 23 km, 6 km, and 6 km respectively for the Odet, Jet and Steir rivers.

TABLE I: Characteristics of the sub-catchments Tréodet, Kerjean, Ty Planche and the whole catchment.

Sub-catchment	Tréodet	Kerjean	Ty Planche
Elevation of the source (IGN69)	175 m	200 m	100 m
Total length of the river (km)	37	21	23
Catchment area (km^2)	205	107	179
Mean streamflow (m^3/s)	4.8	2.27	3.79
10-years flows (m^3/s)	55	19	39
50-years flows (m^3/s)	75	25	53
Max flow 12-2000 (m^3/s)	110	46.6	81
Max flow 12-2013 (m^3/s)	91.5	17.6	42.7
Mean rainfall (mm/year)	743	672	671

III. Data set

The following data sets are used in the study. They all are available from January 2007 to January 2017:

- Spatially distributed observed rainfall and surface temperature data are used as input to the hydrologic model. They respectively come from ANTILOPE (Champeaux et al., 2009) and SAFRAN (Vidal et al., 2010) reanalysis and are available at hourly time step.
- Continuous streamflow measurements come from the French national archive (Banque hydro, http://www.hydro.eaufrance.fr) and are available at the three upstream observing stations (Tréodet, Kerjean, Ty-Planche) at hourly time step. The data are used for hydrologic and hydraulic models calibration.
- Continuous water level measurements provided by the SPC VCB are available at three observing stations on the river (Kervir, Moulin-Vert, Justice) and at the downstream boundary of the model (Plaisance) with a time step of 6 minutes. These data are both used for the calibration of the hydraulic model and the determination of the storm surge for the perturbation of the maritime boundary condition when performing the GSA (see VI-B3).

IV. MORDOR-TS hydrologic model

A. Description and calibration

MORDOR-TS (Garçon, 1996; Garavaglia et al., 2017; Rouhier et al., 2017) is a spatialized and continuous conceptual rainfall-runoff hydrologic model. It has 10 parameters calibrated with respect to a multi-objective function using the caRamel genetic algorithm (Le Moine et al., 2015; Monteil et al., 2019). The calibration of the hydrologic parameters is achieved over a 10-year period from 01/01/2007 to 05/31/2017, after a spin-up period of one year.

Three scores are gathered in the multi-objective function: (i) Nash over the entire time series, (ii) Nash over the inter-annual daily regime and (iii) Nash over the empirical cumulative distribution. Table II shows the Nash values after calibration on these three hydrologic signatures.

Catchment	Tréodet	Kerjean	Ty Planche
Nash hourly runoff	0.94	0.95	0.94
Nash daily regime	0.99	0.99	0.99
Nash cumulative distribution	0.99	0.995	0.996

TABLE II: Nash after calibration of MORDOR-TS parameters.

B. Hydrologic Ensemble Forecasts (HEF)

An Hydrologic Ensemble Forecast (HEF) system is setup by perturbating the value of the parameters of MORDOR-TS. A GSA on discharge computed with the MORDOR-TS model has shown that only 8 over the 10 calibrated parameters control the simulated runoff. The Probability Density Functions (PDF) of these 8 uncertain variables are supposed to be uniform $U[V_{min}, V_{max}]$. For each parameter, V_{min} and V_{max} are determined by the realization of a set of calibrations of the MORDOR-TS model over 2 years periods. The ensemble is created with a Halton sequence of 99 members.

V. Mascaret model

The hydraulic model consists in 172 geometrical cross-sections for a total length of 35 km. The resolution of the computational mesh varies between 5 m and 10 m. The vertical discretization of cross sections is 10 cm. After calibration, 12 different zones of friction coefficients are retained (Figure 3). Strickler coefficients are set to values ranging between 15 $m^{1/3}s^{-1}$ and 37 $m^{1/3}s^{-1}$ in the riverbed, and between 1 $m^{1/3}s^{-1}$ and 34 $m^{1/3}s^{-1}$ in the flood plains. The very low value of 1 $m^{1/3}s^{-1}$ compensates for an incomplete knowledge of the topography/bathymetry and for the presence of a bend in the river geometry.

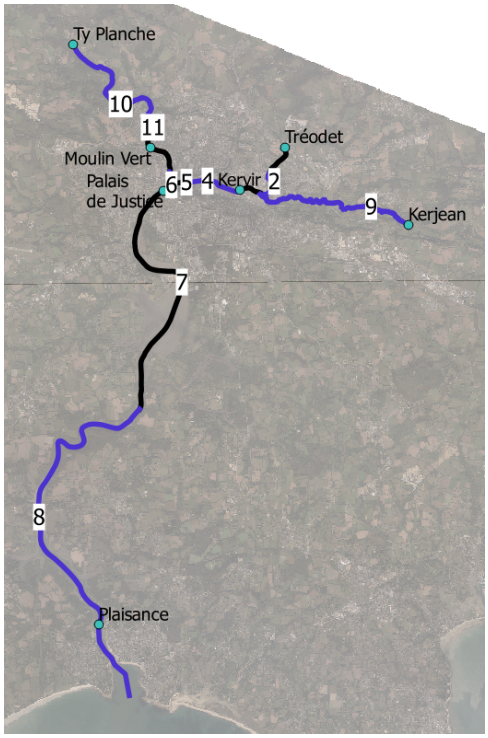

Fig. 3: 12 zones of friction coefficents.

A. Calibration methodology

The hydraulic numerical model was calibrated comparing the simulated water levels over November 1st, 2013 - February 28th, 2014 to observated water level. This winter was characterized by numerous flood events and storm surges. The model was then assessed over November 1st, 2012 - February 28th, 2013. This winter had less storms than the winter used for the calibration.

The cost function is a combination of the RMSE over the whole time series and the RMSE calculated on the value of simulated peaks during extreme events (1):

$$f_C = 0.8 * RMSE_{TimeSerie} + 0.2 * RMSE_{peaks} \quad (1)$$

Figure 4 shows the measured water level at Kervir, Moulin Vert and Justice during the calibration winter. For Kervir and Moulin-Vert, a set of 11 events represented in red are used for the calculation of $RMSE_{peaks}$ in Equation (1). At Justice, the water level is dominated by tide effects, even during river floods. For this location, all the high tide peaks are considered for the calculation $RMSE_{peaks}$. The calculation of $RMSE_{peaks}$ in Equation (1) is thus made on 11 peaks for Kervir and Moulin-Vert, and on about 200 peaks of high tide for Justice.

Fig. 4: Measured water level at Kervir, Moulin Vert and Justice from November 1st, 2013 to February 28th, 2014. Flood and storm surge events are represented in red.

B. Results

Table III shows the results of the calculation of the RMSE for the whole time series during the calibration and the validation winters (respectively denoted "CAL" in black and "VAL" in blue in the table). The green, yellow and orange vigilances correspond to water level classes used for operational forecasting by the SPC VCB. These results show that the performance of the model during the calibration and the validation periods are similar. The model is thus relatively robust.

TABLE III: RMSE (cm) during calibration and validation.

Water height class	Period	Kervir	Moulin-Vert	Justice
All water heights	CAL	2.9	4.8	6.0
	VAL	2.4	4.5	5.3
Green vigilance	CAL	2.6	4.3	6.2
	VAL	2.3	4.4	5.5
Yellow vigilance	CAL	6.0	7.2	5.7
	VAL	6.3	7.2	5.0
Orange vigilance	CAL	3.8	15.46	no data
	VAL	no data	no data	no data

Table IV represents the value of the peaks of the 11 events of the calibration winter and the associated simulated error for Kervir and Moulin-Vert. The value of the peaks are relatively well simulated by the model.

TABLE IV: Value of the peacks of water level for the 11 events of the calibration winter and associated simulated error - Stations Kervir and Moulin-Vert.

Event	Measured water heigth at Kervir (m)	Error (cm)	Measured water heigth at Moulin-Vert (m)	Error (cm)
Dec 2013 - 1	2.72	-4.8	2.07	-1.9
Dec 2013 - 2	1.66	6.7	1.58	8.9
Jan 2014 - 1	2.67	-3.1	2.09	-3.4
Jan 2014 - 2	1.94	3.3	1.93	4.5
Jan 2014 - 3	1.78	3.7	1.58	6.8
Jan 2014 - 4	1.74	-0.6	1.76	6.2
Feb 2014 - 1	2.76	-6.7	2.85	3.2
Feb 2014 - 2	2.35	-0.5	2.26	-5.7
Feb 2014 - 3	2.48	7.1	2.06	0.6
Feb 2014 - 4	2.31	4.6	1.71	5.6
Feb 2014 - 5	1.88	1.3	1.81	2.3

Figure 5 represents the difference between measured and simulated water level for each high tide during the calibration period at Justice. The water level measurement at the moment of the peaks is also represented. A positive value for the peak error corresponds to an overestimation of the model relative to measurements.

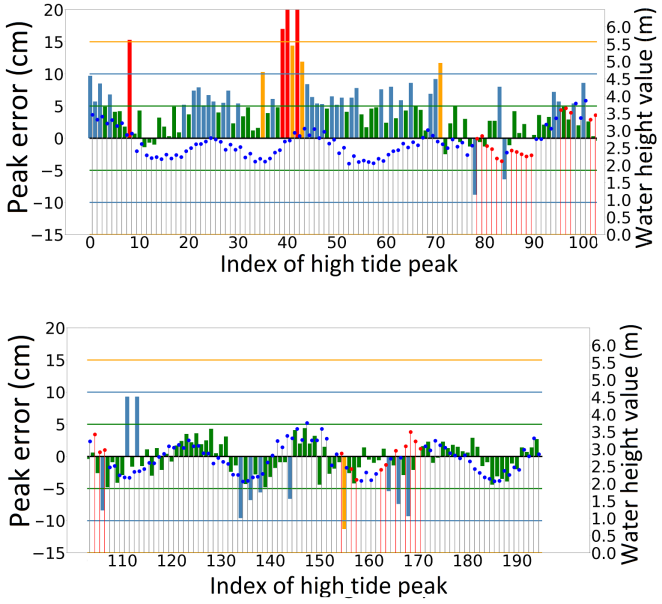

Fig. 5: Peaks errors and associated water level for high tide during 2013-2014 winter - Station Justice.

On this figure, errors are color-coded:

- green corresponds to a difference of less than 5 cm
- blue corresponds to a difference between 5 and 10 cm
- orange corresponds to a difference between 10 and 15 cm
- red corresponds to a difference of more than 15 cm

Figure 5 shows that most of simulated peaks are less than 5 cm of the measures. For only 4 high tides, the model calculates a value with an error more than 15 cm.

VI. Global Sensitivity Analysis (GSA)

A. Variance decomposition and Sobol' indices

Sobol' indices apportion the variance of the output $Y = f(X)$ with $X = (X_1, X_2, ..., X_k)$, to the variation of different inputs $(X_1, ..., X_k)$ on their uncertainty domain. With the assumption that the variance of Y is finite and the input variables are independent, the Hoeffing decomposition (Hoeffding, 1948) provides the relation:

$$V(Y) = \sum_i V_i + \sum_i \sum_{j>i} V_{i,j} + ... + V_{1,2,3,...,K} \quad (2)$$

where

- V_i is the elementary contribution of X_i to V(Y),
- $V_{i,j}$ is the contribution due to interactions between X_i et X_j to V(Y),
- ...
- $V_{1,2,...,k}$ is the contribution due to interaction between all inputs to V(Y).

Dividing Eq. 2 by V(Y) leads to :

$$\sum_i S_i + \sum_i \sum_{j>i} S_{i,j} + ... + S_{1,2,3,...,K} = 1 \quad (3)$$

In (3), S_i is the first order Sobol index which represents the normalized elementary contribution of X_i to V(Y). The total Sobol index representing all contributions related to X_i is defined by:

$$ST_i = S_i + \sum_{i,i\neq j} S_{i,j} + ... + S_{1,2,3,...,K} \quad (4)$$

If they are no interaction between the input parameters, $\sum_i S_i = 1$. In the following, since there are very few interaction between the input parameters, only the first order Sobol' indices will be shown.

B. Uncertainty space for GSA

In order to carry out a GSA on the Mascaret model, we consider three types of uncertain inputs:

- the minor and flood plain friction coefficients for the 12 different zones of the model (Ks_i and Ks_{iM}), represented on figure 3;
- the three hydrologic upstream time series at Tréodet, Kerjean and Ty-Planche (Q);
- the maritime boundary time series (CLMAR).

The quantity of interest Y is the measured water level at a forecast station at a specific time. The GSA is thus applied over time at Kervir, Moulin-Vert and Justice. Scalar uncertain variables are described by their Probability Density Function (PDF) which characteristics are described thereafter.

1) Friction coefficients: The PDFs of friction coefficients are supposed to be uniform. The distribution is centered on the calibrated value with a width of 5 on each side. The values are described in table V.

TABLE V: Distribution of the Strickler coefficients for the GSA

Zone	Ks_{min} minor	Ks_{max} minor	Ks_{min} flood plain	Ks_{max} flood plain
1	25	35	15	25
2	15	25	5	15
3	10	20	5	15
4	33	43	8.5	18.5
5	13	17	5	15
6	31.5	41.5	29	39
7	32	42	20	30
8	20.5	30.5	1	10
9	15	25	5	15
10	15	25	5	15
11	27.5	37.5	1	10
12	17.5	22.5	5	15

2) Hydrologic input: The HEF described in section IV-B provides 99 members of hydrologic time series. The uncertainty in the hydrologic input is thus represented by an index drawn uniform between 1 and 99.

3) Maritime boundary condition: The water heigth at the downstream maritime boundary condition is time-dependent. The sampling procedure must thus preserve the temporal correlation of errors.

The time varying pertubation is applied on the storm surge s. The perturbation is supposed to be a Gaussian Process with a Gaussian covariance function C. The correlation length is arbitrary set to 6 hours, which is the duration of a half tide. The amplitude of the covariance function C is chosen in order to set the median standard deviation of the perturbed storm surge to about 18 cm, which is approximatively the median standard deviation of the measured tide surge. s is written as a Karhunen-Loève decomposition as the truncated form of n_p orthogonal functions where the mode coefficients ϵ_i are independent standard normal variables:

$$s(t) = \sum_{i=0}^{n_p} \sqrt{\lambda_i}\phi_i(t)\epsilon_i. \quad (5)$$

λ_i and ϕ_i are respectively the eigenvalues and the eigenfunctions of the covariance function, i.e. solutions of the Fredholm equation:

$$\int C(t_1, t_2)\phi_i(t_2)dt_2 = \lambda_i\phi_i(t_1). \quad (6)$$

A set of 99 perturbed storm surge time series are generated with a sampling of ϵ_i. The uncertainty in the maritime boundary condition input is thus represented by an index drawn uniform between 1 and 99.

4) Comparison of the standard deviation of upstream and donwstream perturbations: Figure 6 represents the standard deviation of the upstream and downstream perturbations. On this figure, upstream streamflows have been converted into water level by their rating curve. It should be noted that the magnitude of the imposed perturbations are of the same order for the four boundary conditions.

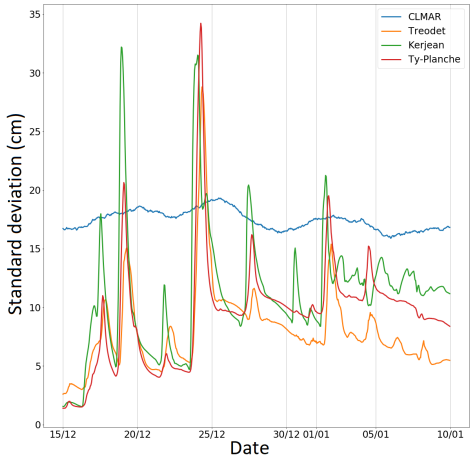

Fig. 6: Standard deviation of the upstream and dowstream perturbations (cm)

VII. Results and discussion

A GSA is carried out for four different configurations:

- Configuration 1: the values of the minor friction coefficients of the 12 zones are perturbed. The aim of this study is to determine the impact of the spatially distributed minor friction coefficients. The Sobol' indices are computed with 20800 perturbed simulations.
- Configuration 2: only the 6 zones which mainly control the simulated water level at the three stations are considered. These zones are determined thanks to the previous study (configuration 1). The minor and flood plain friction coefficients are now perturbed. The aim of this study is to determine the impact of flood plain friction coefficients. The Sobol' indices are calculated with 20800 perturbed simulations.
- Configuration 3: the same 6 zones as in configuration 2 are considered, but again only with a perturbation of minor friction coefficients. In addition, the hydrologic inputs and the maritime boundary condition are also taken into account. The aim of this study is to determine the impact of the forcings against the friction coefficients. The Sobol' indices are computed with 30600 perturbed simulations.
- Configuration 4: the same 6 zones as in configuration 2 and 3 are considered with a perturbation of both minor and flood plain friction coefficients. The hydrologic inputs and the maritime boundary condition are also taken into account. The aim of this study is to determine the impact of the forcings against the minor and flood plain friction coefficients. The Sobol' indices are computed with 48000 perturbed simulations.

For each configuration, the value of the friction coefficients are perturbed according to the ranges described in table V. The results are achieved for the event from the 23 to the 26 December

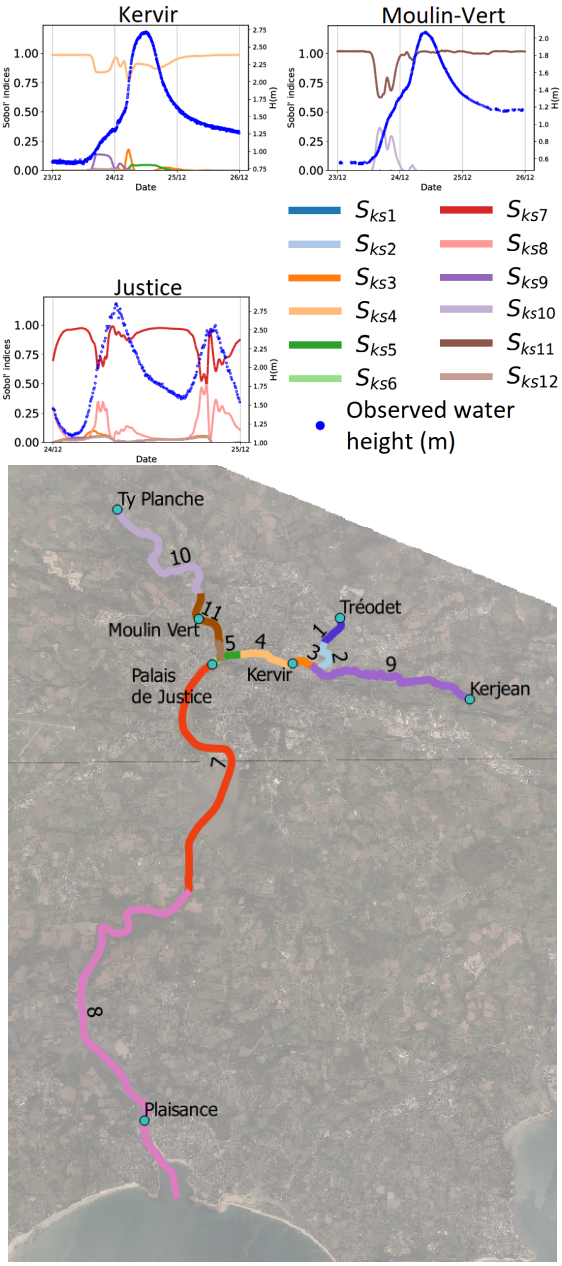

Fig. 7: Configuration 1: Sobol' indices time series and associated zones for the event from the 23 to the 26 December, 2013

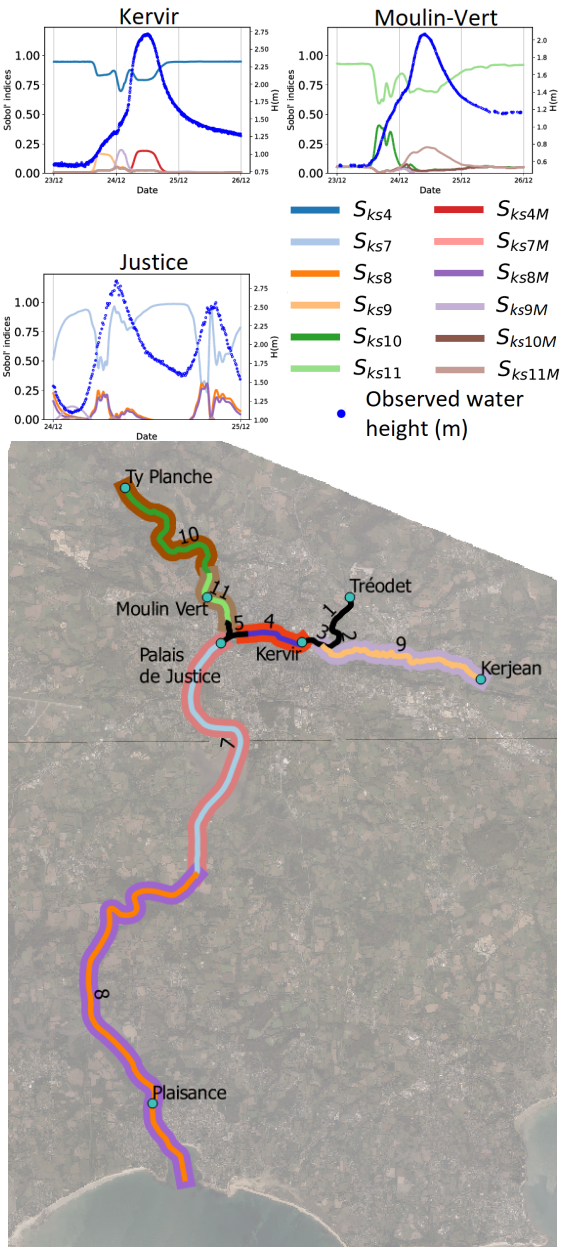

Fig. 8: Configuration 2: Sobol' indices time series and associated zones for the event from the 23 to the 26 December, 2013

2013. The computation of Sobol' indices is realized thanks to the python modules OpenTURNS (http://openturns.org/) and Batman (Roy et al., 2018).

A. Configuration 1: impact of spatially distributed minor friction coefficients

Figure 7 shows the Sobol' indices time series during the event. These graphics highlight that for Kervir and Moulin-Vert, the simulated water level is mainly controlled by the downstream Strickler friction coefficient: Ks_4 for Kervir and Ks_{11} for Moulin-Vert. To a lesser extent, the upstream Strickler friction coefficient slightly controls the simulated water level during the beginning of the flood and the end of the redecending water level: Ks_9 for Kervir and Ks_{10} for Moulin-Vert.

The behavior is different at Justice: the simulated water level is mainly controlled by the just downstream Strickler friction coefficient Ks_7. But it is also cyclically controlled by Ks_8 according the tide level, the zone 8 being situated immediately downstream the zone 7. The value of the upstream Strickler friction coefficients have no impact on the simulated level at Justice.

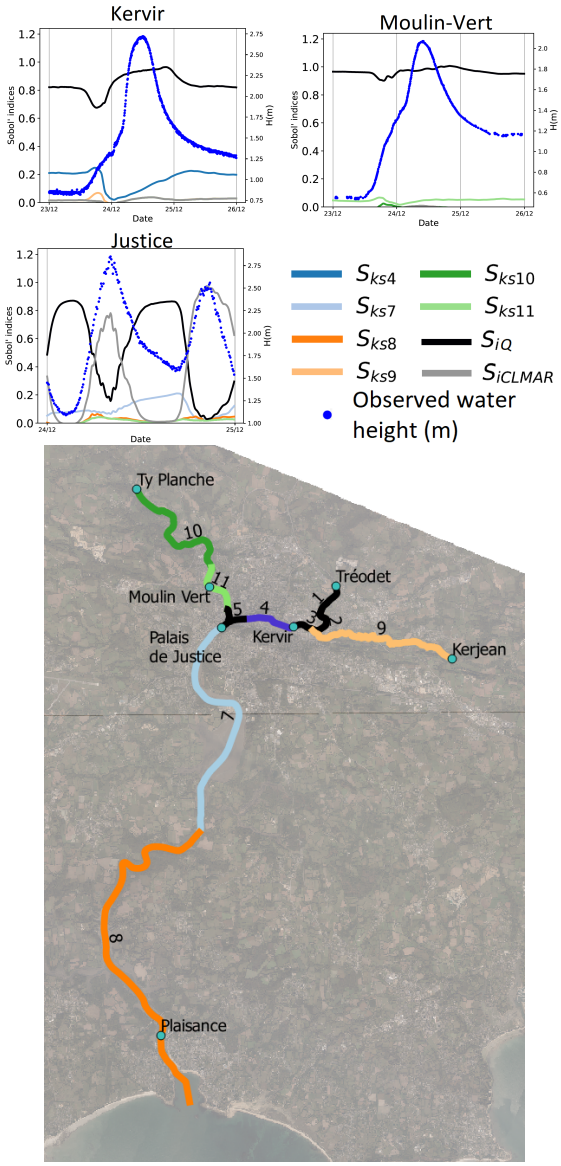

Fig. 9: Configuration 3: Sobol' indices time series and associated zones for the event from the 23 to the 26 December, 2013

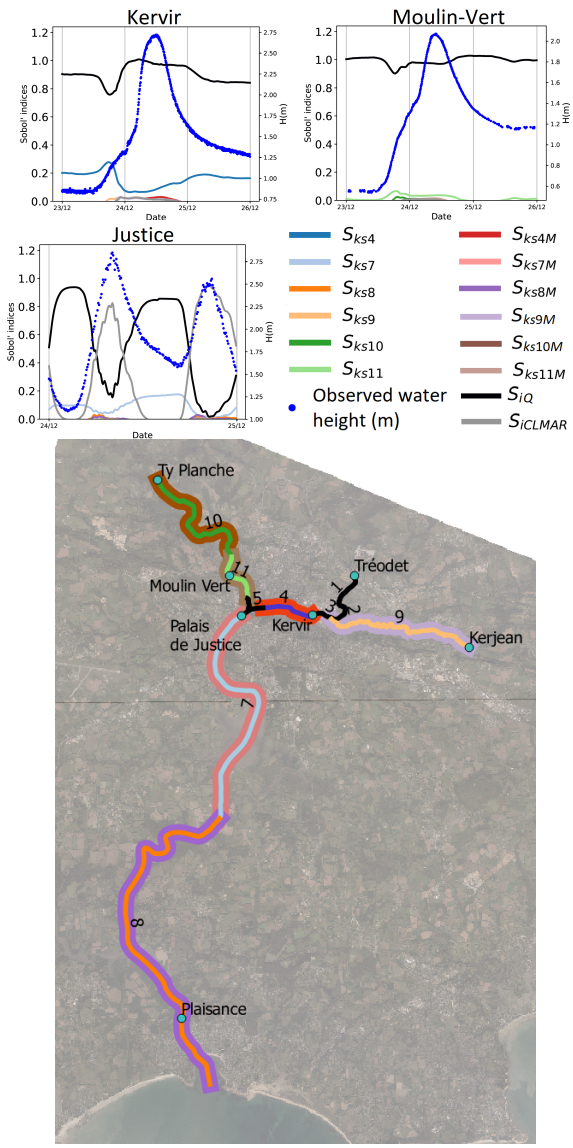

Fig. 10: Configuration 4: Sobol' indices time series and associated zones for the event from the 23 to the 26 December, 2013

B. Configuration 2: impact of flood plain friction coefficients

In this second study, we consider the minor and flood plain friction coefficients of the 6 zones which mainly control the simulated water level at the three stations: zones 4, 7, 8, 9, 10 and 11. Figure 8 shows the Sobol' indices time series during the event.

At Kervir, the water level is still controlled by the value of the minor Strickler coefficient of the downstream zone Ks_4. Simultaneously with the peak of water level, the value of the flood plain Strickler coefficient Ks_{4M} increases in importance. This corresponds to the moment when the floodplain is activated. The upstream zone 9 maintains a little influence at the beginning of the event, firstly with the minor coefficient Ks_9, and then with the flood plain coefficient Ks_{9M}.

Moulin-Vert shows similar characteristics, with a main control by Ks_{11} minor, and Ks_{11M} activated around the peak of the event. At the beginnning of the event, the minor upstream coefficient Ks_{10} has some influence.

At Justice, the same trend as the previous study (configuration 1) is found regarding the minor coefficient Ks_7. However, the flood plain is not activated here since the Sobol index of Ks_{7M} is unsignificant. This result is consistent with the sections geometry in this zone. Both minor and flood plain coefficients of the zone 8 are important when the water level is rising. The zone 8 corresponds to an esturary zone. The flood plain considered in the model is in fact activated at each tide cycle when the tide rises.

C. Configuration 3: impact of forcings against minor friction coefficients

In this third study, we consider the same 6 zones as in configuration 2 where friction coefficients mainly control the simulated water level at the three stations: zones 4, 7, 8, 9, 10 and 11. Only the minor friction coefficients are considered. In addition, we also take into account the hydrologic inputs and the maritime boundary condition. Figure 9 shows the Sobol' indices time series for the three forecast stations during the event.

At Kervir and Moulin-Vert, it is overall the choice of the hydrologic scenario which determines the simulated water level. It should be noted that at Moulin-Vert, the downstream friction coefficient has almost no influence. This trend is a little less marked during other events.

At Justice, the influence of the minor Strickler coefficient Ks_8 remains significant, yet the water level is largely dominated by the choice of the hydrologic and the maritime boundary condition scenarios. When the levels are high, the maritime boudary condition is for a large part responsible for the simulated water level, and on the contrary, when the levels are low, the hydrologic scenario mainly controls the simulated water level.

D. Configuration 4: impact of forcings against minor and flood plain friction coefficients

In this last study, we consider the minor and flood plain coefficients of the 6 zones where friction coefficients mainly control the simulated water level at the three stations: zones 4, 7, 8, 9, 10 and 11. The hydrologic inputs and the maritime boundary condition are also taken into account. Figure 10 shows the Sobol' indices time series for the three forecast stations during the event.

This graphs highlith that the flood plain friction coefficients are not very influent, since the Sobol'indices time series are almost identical to those of the configuration 3. However, we note a slight influence of the flood plain coefficient Ks_{11} at Moulin-Vert during other events (not shown here).

VIII. Conclusion

The Mascaret model of the Odet river, daily used by the SPC VCB for flood forecasting, was studied through a Global Sensitivity Analysis (GSA). It provides Sobol' indices that rank the uncertainty sources. GSA shows that if the boundary conditions are not perturbed, the simulated water level at the stations are mainly controlled by the immediate downstream friction coefficient. The flood plains are activated around the peak of the events and then the flood plain Strickler friction coefficients become important. GSA also shows that if perturbed, the boundary conditions are decisive for the simulated water level.

In further work, the results of the GSA study will be used for the realization of Hydraulic Ensemble Forecasts, and for correcting the simulation chain by data assimilation.

IX. Acknowledgements

The authors would like to thank the French national service for flood forecasting (SCHAPI) for supporting this study. They also would like to thank EDF-DTG for the fourniture of the MORDOR-TS hydrologic model and Fabrice Zaoui (EDF R&D) for the interfacing python module pymordor. The authors also acknowledge the Pôle de Calcul et de Données Marines (PCDM) for providing DATARMOR storage and computational resources. URL: http://www.ifremer.fr/pcdm.

References

Champeaux, J.L., Dupuy, P., Laurantin, O., Soulan, I., Tabary, P., Soubeyroux, J.M., 2009. Les mesures de précipitations et l'estimation des lames d'eau à Météo-France : état de l'art et perspectives. La Houille Blanche , 28–34doi:10.1051/lhb/2009052.

Garavaglia, F., Le Lay, M., Gottardi, F., Garçon, R., Gailhard, J., Paquet, E., Mathevet, T., 2017. Impact of model structure on flow simulation and hydrological realism: from a lumped to a semi-distributed approach. Hydrology and Earth System Sciences 21, 3937–3952. doi:10.5194/hess-21-3937-2017.

Garçon, R., 1996. Prévision opérationnelle des apports de la Durance à Serre-Ponçon à l'aide du modèle MORDOR. Bilan de l'année 1994-1995. La Houille Blanche , 71–76doi:10.1051/lhb/1996056.

Hoeffding, W., 1948. A Class of Statistics with Asymptotically Normal Distribution. The Annals of Mathematical Statistics 19, 293–325. doi:10.1214/aoms/1177730196.

Le Moine, N., Hendrickx, F., Gailhard, J., Garçon, R., Gottardi, F., 2015. Hydrologically Aided Interpolation of Daily Precipitation and Temperature Fields in a Mesoscale Alpine Catchment. Journal of Hydrometeorology 16, 2595–2618. doi:10.1175/JHM-D-14-0162.1.

Monteil, C., Zaoui, F., Le Moine, N., Hendrickx, F., 2019. Technical note: the caRamel R package for Automatic Calibration by Evolutionary Multi Objective Algorithm. Hydrology and Earth System Sciences Discussions 2019, 1–16. doi:10.5194/hess-2019-259.

Rouhier, L., Le Lay, M., Garavaglia, F., Le Moine, N., Hendrickx, F., Monteil, C., Ribstein, P., 2017. Impact of mesoscale spatial variability of climatic inputs and parameters on the hydrological response. Journal of Hydrology 553, 13–25. doi:10.1016/j.jhydrol.2017.07.037.

Roy, P., Ricci, S., Dupuis, R., Campet, R., Jouhaud, J.C., Fournier, C., 2018. BATMAN: Statistical analysis for expensive computer codes made easy. The Journal of Open Source Software 3, 493. doi:10.21105/joss.00493.

Vidal, J.P., Martin, E., Franchistéguy, L., Baillon, M., Soubeyroux, J.M., 2010. A 50-year high-resolution atmospheric reanalysis over France with the Safran system. International Journal of Climatology 30, 1627–1644. doi:10.1002/joc.2003.